

Kibdelones: Novel Anticancer Polyketides from a Rare Australian Actinomycete

Ranjala Ratnayake,^[a] Ernest Lacey,^[b] Shaun Tennant,^[b] Jennifer H. Gill,^[b] and Robert J. Capon*^[a]

Abstract: The kibdelones are a novel family of bioactive heterocyclic polyketides produced by a rare soil actinomycete, *Kibdelosporangium* sp. (MST-108465). Complete relative stereostructures were assigned to kibdelones A–C (**1–3**), kibdelone B rhamnoside (**5**), 13-oxokibdelone A (**7**), and 25-methoxy-24-oxokibdelone C (**8**) on the basis of detailed spectroscopic analysis and chemical interconversion, as well as mechanistic and biosynthetic consider-

ations. Under mild conditions, kibdelones B (**2**) and C (**3**) undergo a facile equilibration to kibdelones A–C (**1–3**), while kibdelone B rhamnoside (**5**) equilibrates to a mixture of kibdelone A–C rhamnosides (**4–6**). A plausible mechanism for this equilibration is pro-

posed and involves air oxidation, quinone/hydroquinone redox transformations, and a choreographed sequence of keto/enol tautomerizations that aromatize ring C via a quinone methide intermediate. Kibdelones exhibit potent and selective cytotoxicity against a panel of human tumor cell lines and display significant antibacterial and nematocidal activity.

Keywords: actinomycete • anti-tumor agents • natural products • NMR spectroscopy • polyketides

Introduction

During our investigations into bioactive metabolites from Australian microorganisms we examined an isolate of a rare actinomycete genus, *Kibdelosporangium* sp. (MST-108465). Bioassay profiling of a methanolic extract derived from a culture of MST-108465 uncovered an unusual combination of potent antibacterial, nematocidal, and cytotoxic activities. HPLC-DAD-ELSD (DAD = diode array detector; ELSD = evaporative light scattering detector) analysis of the secondary metabolites present drew attention to a family of non-polar metabolites displaying distinctive UV-visible spectra.

An electronic search of an in-house database (MST, COMET)^[1] comprising HPLC-DAD-ELSD profiles from over 1500 natural products, and extracts from 6000 annotated microorganisms (a comprehensive library of microbes that produce microbial metabolites from across the spectrum of known structure classes), failed to identify these nonpolar metabolites. A further search against a larger COMET data set comprising HPLC-DAD-ELSD profiles from 50000 microbes selected for their capacity to yield novel secondary metabolites also failed to return a match.

Taken together, these searches suggested that *Kibdelosporangium* sp. (MST-108465) and its metabolites were remarkably rare. Scaled up solid and liquid-phase fermentation of the *Kibdelosporangium* sp. optimized for production of cytotoxic metabolites yielded a family of new heterocyclic polyketides exemplified by kibdelone A (**1**). In this report we describe the isolation, characterization, structure elucidation, and biological evaluation of kibdelones A–C (**1–3**), kibdelone B rhamnoside (**5**), 13-oxokibdelone A (**7**), and 25-methoxy-24-oxokibdelone C (**8**).

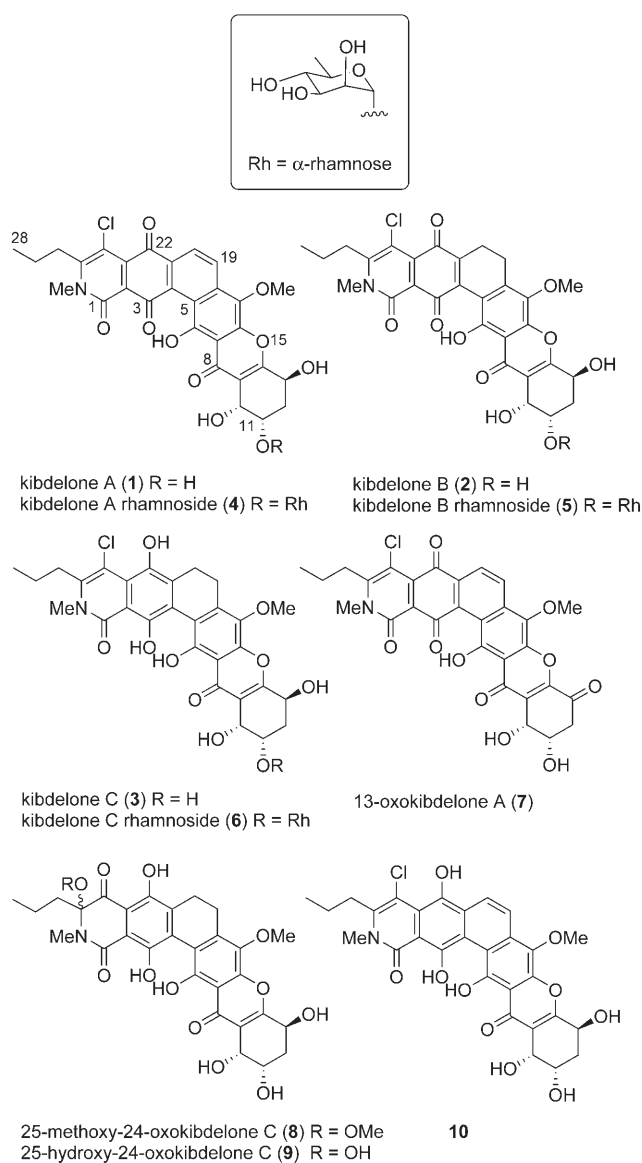
[a] R. Ratnayake, Prof. R. J. Capon
Centre for Molecular Biodiversity
Institute for Molecular Bioscience
University of Queensland, St. Lucia
QLD, 4072 (Australia)
Fax: (+94) 7-3346-2090
E-mail: r.capon@imb.uq.edu.au

[b] Dr. E. Lacey, Dr. S. Tennant, Dr. J. H. Gill
Microbial Screening Technologies Pty. Ltd.
Building A, 28–54 Percival Road, Smithfield
NSW, 2164 (Australia)

Supporting information for this article (NMR assignments for compounds **2–8** and **10**, fermentation media treatment/extraction methods, and kibdelones A–C equilibration studies) is available on the WWW under <http://www.chemeurj.org/> or from the author.

Results and Discussion

Fermentation and isolation: Having established that the MeOH extract obtained from a solid-phase microfermenta-



tion of *Kibdelosporangium* sp. (MST-108465) was rich in novel structurally diverse bioactive metabolites, a spore suspension was used to inoculate two solid (ISP2 agar and barley grain) and two liquid (ISP2 and rice flour) media. In all cases, the cellular biomass and culture media were extracted with MeOH to generate crude extracts, which then underwent chemical and biological profiling to confirm and correlate the production and diversity of bioactive metabolites—defining conditions for the optimized production of differing suites of bioactive *Kibdelosporangium* sp. metabolites. Prefractionation of the combined extracts by using solvent partitioning and preparative C_{18} solid-phase extraction (SPE) returned a MeOH eluting fraction (875 mg) enriched in bioactive metabolites that subsequently underwent preparative C_{18} and C_8 HPLC fractionation to yield an array of 100 fractions. Bioassays carried out on these fractions localized the antibacterial (*Bacillus subtilis*, LD_{99} = 1–11 $\mu\text{g mL}^{-1}$), nematocidal (*Haemonchus contortus*, LD_{99} 3–

10 $\mu\text{g mL}^{-1}$), and cytotoxic (NS-1, LD_{99} = 1–11 $\mu\text{g mL}^{-1}$) activities in those fractions that contained kibdelones. This report details our investigations into these bioactive *Kibdelosporangium* sp. fractions.

Solvent partitioning of the bioactive fractions, followed by C_{18} and C_8 SPE and semipreparative HPLC, yielded a new class of bioactive polyketides exemplified by kibdelones A–C (1–3). Chemical and biological profiling obtained during the fermentation studies (see above) indicated that solid-phase barley fermentation optimized the production of kibdelones. In an attempt to both increase production levels and access additional “kibdelone related co-metabolites” detected as very minor components in earlier fermentations, we undertook a scaled up solid-phase fermentation of *Kibdelosporangium* sp. on barley (7 \times 500 g barley, incubated for 18 d at 28°C). The resulting fermentation product was extracted with MeOH (7 \times 1.5 L) and concentrated in vacuo, then partitioned with EtOAc (2.6 L). Prefractionation of half of the EtOAc concentrate (4 g) by C_{18} SPE, and multiple elution through preparative C_{18} and C_8 HPLC, returned kibdelone A (1; 29 mg, 0.60%), kibdelone B (2; 52 mg, 1.1%), kibdelone C (3; 97 mg, 2.0%), and kibdelone B rhamnoside (5; 5.2 mg, 1.1%), as well as the minor analogues 13-oxokibdelone A (7; 0.9 mg, 0.02%) and 25-methoxy-24-oxokibdelone C (8; 2.8 mg, 0.06%), and traces of 25-hydroxy-24-oxokibdelone C (9)—the latter two compounds were speculated to be artifacts derived from solvolysis of kibdelone B (see below). At this time, we report the structure elucidation and biological properties of the kibdelones.

Structure elucidation: The HRESI(+)-MS data for kibdelone A (1) displayed a pseudo molecular ion consistent with a molecular formula ($C_{29}H_{24}^{35}ClNO_{10}$, $\Delta m_{\text{mu}} = 1.0$) requiring 18 double-bond equivalents (DBE). Initial examination of the UV and ^1H NMR spectroscopic data indicated a highly aromatic molecular structure, featuring both O and N methyls, three secondary alcohols, a chelated phenol, and a pair of *ortho*-coupled aromatic protons. Careful analysis of the 1D and 2D NMR spectroscopic data (Table 1) revealed correlation sequences consistent with the structure fragments highlighted in Figure 1. A detailed account of these assignments is given below.

A sequence of COSY and gHMBC correlations from C-8 to C-14 defined the structure fragment incorporating ring F. Attachment of O-15 to C-14 in this fragment was inferred from the ^{13}C NMR shift for this carbon atom ($\delta_{\text{C}} = 166.3$ ppm), while the deshielded character of C-8 ($\delta_{\text{C}} = 183.7$ ppm) identified it as a carbonyl. A sequence of COSY and gHMBC correlations from C-28 to C-24 defined the structure fragment for an *n*-propyl side chain attached to a fully substituted double bond ($\delta_{\text{C}} = 105.7$ and 156.41 ppm). The deshielded ^{13}C NMR shift for C-25 ($\delta_{\text{C}} = 156.41$ ppm) supported attachment of the N–Me (see below), while the shielded character of C-24 ($\delta_{\text{C}} = 105.7$ ppm) was consistent with chlorine substitution. ROESY correlations from H_2 -26 and H_2 -27 to the N–Me confirmed the spatial proximity of

Table 1. NMR spectroscopic ($[D_6]DMSO$, 600 MHz) assignments for kibdelone A (**1**).

	$^1H \delta_H$ m (J [Hz])	^{13}C	COSY	gHMBC
1		156.36		
2		121.0 ^[a]		
3		180.8 ^[a]		
4		133.6		
5		113.2		
6		156.6		
7		106.9		
8		183.7		
9		117.0		
10	4.73 m	61.4	H-12a, H-11, 10-OH	C-14, C-12, C-11, C-9, C-8
11	3.95 ddd (12.4, 6.0, 3.1)	64.0	H-12, H-10, 11-OH	
12a	2.26 ddd (13.0, 12.4, 4.4)	33.8	H-13, H-12b, H-11, H-10	C-11, C-10
12b	1.79 br d (13.0)		H-12a, H-11	C-14, C-13, C-10
13	4.71 m	65.2	H-12a, 13-OH	C-14, C-12, C-11, C-9
14		166.3		
15 [O]				
16		145.5 ^[a]		
17		133.3		
18		137.6		
19	8.38 d (9.0)	125.8	H-20	C-21, C-18, C-17, C-5
20	8.11 d (9.0)	124.3	H-19	C-22, C-19, C-18, C-4
21		131.4		
22		181.3		
23		138.7 ^[a]		
24		105.7		
25		156.41		
26	3.02 br dd (8.2, 8.0)	33.1		C-28, C-27, C-1, C-24
27	1.64 m	19.6		C-28, C-26, C-25
28	1.06 t (7.2)	13.9		C-27, C-26
OMe	4.02 s	62.2		C-17
NMe	3.67 s	33.2		C-26, C-25/C-1
6 OH	14.23 s			C-7, C-6, C-5
10 OH	5.07 d (5.3)		H-10	C-10, C-9
11 OH	4.79 d (6.0)		H-11	C-12, C-11, C-10
13 OH	6.11 d (6.3)		H-13	C-14, C-13, C-12

[a] Assignments are made in comparison with literature data and co-metabolites.

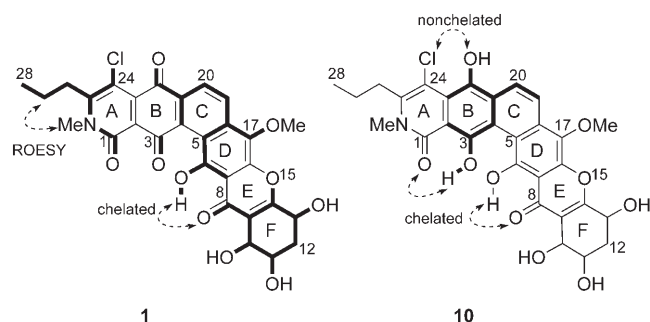


Figure 1. 2D NMR connectivity sequences for structure fragments and key through-space correlations for kibdelone A (**1**) and its reduction product **10**.

these functionalities (including N–Me substitution to C-25), while a gHMBC correlation from the N–Me to C-1 ($\delta_C = 156.36$ ppm) extended this structure fragment to include an amide/lactam moiety. The set of gHMBC correlations about H-19 and H-20 clearly defined the tetrasubstituted ring C, and positioned the quaternary C-22 and C-17 as shown. That C-22 was incorporated into a carbonyl (quinone) was apparent from the ^{13}C NMR shift ($\delta_C = 180.7$ ppm), while a

correlation from the O–Me to C-17 positioned the methoxy moiety as shown. Further to this, gHMBC correlations from the 6-OH to C-5, C-6, and C-7 positioned the phenol on the fully substituted ring D as indicated, and required placement of a coplanar C-8 carbonyl to achieve chelation—as indicated by the highly deshielded and sharp 1H NMR resonance for 6-OH ($\delta_H = 14.23$ ppm)—and thereby defined the regiochemistry of the ring E/F fusion. The upfield ^{13}C NMR chemical shift for the C-1 lactam carbonyl ($\delta_C = 156.36$ ppm) was consistent with it being *peri* to a carbonyl/quinone (compare xantholipin)^[2] as opposed to the sp^2 -hybridized carbon atom of a hydroquinone (compare actinoplanones and simaomicin).^[3,4,5] The ^{13}C NMR shift for one of the remaining unassigned carbon atoms was indicative of a quinone ($\delta_C = 183.4$ ppm), and was attributed to C-3—thereby defining ring B as a *p*-quinone. The four structure fragments described in Figure 1 account for all but three quaternary sp^2 carbon

atoms. The deshielded nature of one of these unassigned carbon atoms ($\delta_C = 145.5$ ppm) required that it be substituted by oxygen and positioned at C-16, completing the fusion between rings D and E. This ring D/E linkage also explained the chelated character of the C-6 hydroxyl. The two remaining carbon atoms were attributed to C-2 ($\delta_C = 121.0$ ppm) and C-23 ($\delta_C = 138.7$ ppm). Final assembly of the total structure for kibdelone A (**1**) presented a challenge, as the available data did not unambiguously differentiate between the structure as shown and an isomer with an alternative regiochemistry about the ring A/B junction. This issue was successfully resolved by NMR spectroscopic analysis (see the Supporting Information) of the hydroquinone **10** obtained by the in situ (NMR tube) reduction of kibdelone A (**1**) with sodium dithionite. The 1H NMR spectrum of dihydrokibdelone A (**10**) displayed downfield resonances for two chelated phenolic protons, 3-OH ($\delta_H = 14.69$ ppm) and 6-OH ($\delta_H = 14.11$ ppm) and one nonchelated phenolic proton, 22-OH ($\delta_H = 9.23$ ppm)—as would be predicted from the structure as shown. A set of gHMBC correlations (see Figure 1 and the Supporting Information) from **10** the nonchelated phenolic resonance (22-OH) to C-21 ($\delta_C = 129.1$ ppm), C-22 ($\delta_C = 137.6$ ppm), and C-23 ($\delta_C =$

120.6 ppm); 2) a chelated phenolic resonance (3-OH) to C-2 ($\delta_{\text{C}}=108.7$ ppm), C-3 ($\delta_{\text{C}}=153.9$ ppm), and C-4 ($\delta_{\text{C}}=114.7$ ppm); and 3) the ring C aromatic protons H-20 to C-4 ($\delta_{\text{C}}=114.7$ ppm) and C-22 ($\delta_{\text{C}}=137.6$ ppm) and H-19 to C-21 ($\delta_{\text{C}}=129.1$ ppm), all supported the connectivity of rings A and B in **1** and **10** as shown. Further evidence for the placement of the quinone (ring B) in kibdelone A (**1**), as opposed to a connectivity of ring A with the hydroquinone (ring D) comes from the ^{13}C NMR chemical shift for C-1 ($\delta_{\text{C}}=165.7$ ppm) in **10**, which was deshielded relative to **1** (C-1, $\delta_{\text{C}}=156.36$) as predicted by literature precedence.^[5]

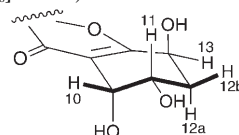
HRESI(+)-MS analysis of kibdelone B (**2**) revealed a pseudo molecular ion consistent with a molecular formula ($\text{C}_{29}\text{H}_{26}^{35}\text{ClNO}_{10}$, $\Delta\text{mmu}=-1.5$) requiring 17 DBE, and indicative of a dihydro analogue of kibdelone A (**1**). While it was tempting to speculate that kibdelone B (**2**) was the hydroquinone analogue **10** prepared by reduction of **1**, this proved to not be the case, with the ^1H NMR spectroscopic data for **2** displaying only a single chelated phenolic OH attributable to 6-OH. Although isomeric with **10**, the NMR spectroscopic data for kibdelone B (**2**) differed significantly, featuring replacement of the aromatic methines H-19 and H-20 with mutually coupled methylenes ($\delta_{\text{H}}=2.87$ and $\delta_{\text{C}}=21.5$ ppm; $\delta_{\text{H}}=2.63$ and $\delta_{\text{C}}=18.4$ ppm)—consistent with reduction of $\Delta^{19,20}$. Detailed 2D NMR spectroscopic analysis of kibdelone B (**2**) (see the Supporting Information) revealed correlation sequences consistent with those observed for kibdelone A (**1**), and supported the structure as assigned (less stereochemistry). Unambiguous confirmation of the structure assigned to kibdelone B (**2**) was obtained on chemical interconversion with kibdelone A (**1**) (see below).

HRESI(+)-MS analysis of kibdelone C (**3**) revealed a pseudo molecular ion consistent with a molecular formula ($\text{C}_{29}\text{H}_{28}^{35}\text{ClNO}_{10}$, $\Delta\text{mmu}=-4.0$) requiring 16 DBE, and indicative of a dihydro analogue of kibdelone B (**2**). On this occasion, the appearance in the ^1H NMR spectrum of two chelated ($\delta_{\text{H}}=13.99$ and 13.14 ppm) and one nonchelated ($\delta_{\text{C}}=8.42$ ppm) phenolic OH was suggestive that ring B in **3** was at the hydroquinone oxidation level. This observation was further supported by a diagnostic downfield shift for the N-Me lactam carbonyl carbon atom ($\delta_{\text{C}}=165.0$ ppm).^[5] Detailed 2D NMR spectroscopic analysis of kibdelone C (**3**) (see the Supporting Information) revealed correlation sequences consistent with those observed for kibdelone A (**1**), and supported the structure as assigned (less stereochemistry). Once again, unambiguous confirmation of the structure assigned to kibdelone C (**3**) was obtained on chemical interconversion with kibdelone A (**1**) (see below).

To confirm the regiochemistry and assign a relative stereochemistry about C-10, C-11, and C-13 in all kibdelones required careful analysis and interpretation of the ^1H NMR data about ring F. Unfortunately, for kibdelones A (**1**) and B (**2**) this analysis was problematic as the ^1H NMR resonances for H-10 and H-13 overlapped. Fortunately, these two resonances were well resolved for kibdelone C (**3**), and as kibdelones A–C undergo a facile equilibration (see below), structural assignments in ring F for **3** can be directly attrib-

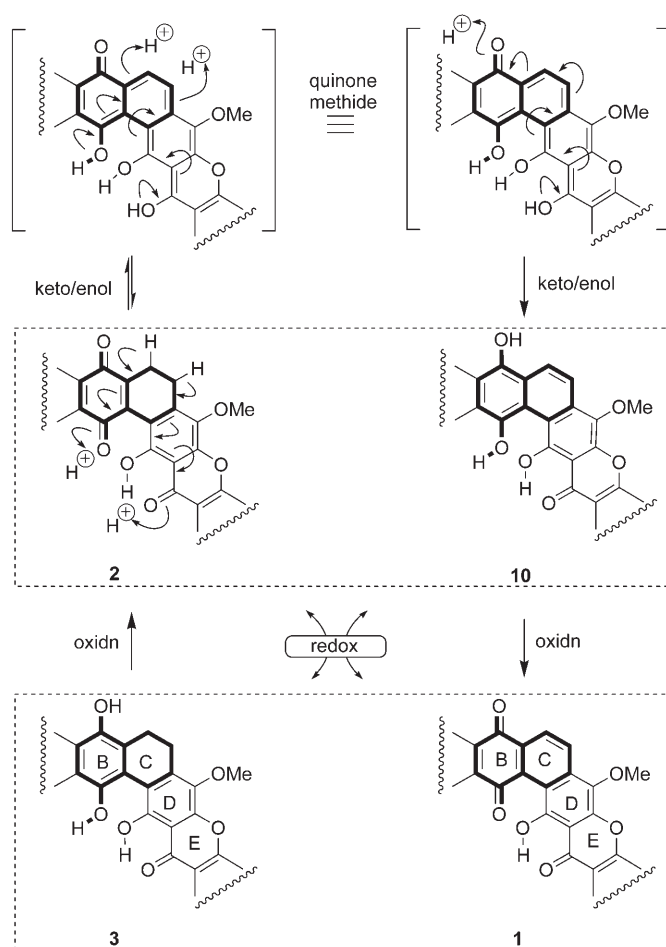
uted to **1** and **2**. Detailed NMR spectroscopic analysis of ring F in **3** required unambiguous assignment of ^1H NMR resonances for H-10 and H-13. In the gHMBC spectrum for **3**, a pair of strong 3-bond correlations from the resonance at $\delta_{\text{H}}=4.70$ ppm to C-8 and C-14 unambiguously assigned H-10, while a 3-bond correlation from $\delta_{\text{H}}=4.67$ ppm to C-9 assigned H-13. With the remaining ring F hydroxymethine ($\delta_{\text{H}}=3.93$ ppm) displaying strong COSY correlations to H-10 and H₂-12, the final ring F hydroxy was positioned at C-11, thereby confirming the kibdelone ring F regiochemistry as shown. Values for $J(11,12a)$ and $J(12a,13)$ of 12.0 and 4.5 Hz clearly indicated pseudodiaxial and -axial-equatorial relationships, and required placement of the C-11 and C-13 hydroxyls in pseudoequatorial and -axial orientations, respectively. Likewise, a value for $J(10,11)$ of 3.9 Hz suggested placement of the C-10 hydroxyl in a pseudoaxial orientation. Supportive of this relative stereochemistry was a small long range coupling between H-10 and H-12b ($J(10,12b)=1.0$ Hz), indicative of a coplanar W coupling (Table 2). In this way the relative stereochemistry for kibdelones A–C (**1–3**) can be assigned as shown.

Table 2. ^1H NMR ($[\text{D}_6]\text{DMSO}$) J values for kibdelone C (**3**).



	J [Hz]		J [Hz]
$J(10,11)$	3.9	$J(12a,12b)$	13.3
$J(10,12b)$	≤ 1.0	$J(12a,13)$	4.5
$J(11,12a)$	12.0	$J(12b,13)$	1.8
$J(11,12b)$	3.0		

On standing at room temperature a MeOH solution of kibdelone B (**2**) was noted to slowly change color from orange to a greenish yellow, a process that was accelerated on heating. A similar transformation (bright yellow to greenish yellow) was also observed for a MeOH solution of kibdelone C (**3**). Concerned about the stability of the kibdelones, we undertook an HPLC-DAD-MS analysis of MeOH solutions of purified **1**, **2**, and **3** at 40°C, which revealed that while **1** was stable to these conditions, **2** and **3** underwent conversion over 18 h to a common equilibrium mixture (**1/2/3** in a ratio of 3:1:2)—with the rate of equilibration being in the order kibdelone B > kibdelone C. Intrigued by this process, we were keen to propose a plausible mechanism that would both explain the phenomena and provide insights to control and even exploit this transformation. Key to explaining this equilibration process was the need to provide a mechanism for changing the oxidation levels for ring C in kibdelones B and C, compared to kibdelone A. Our proposed mechanism outlined in Scheme 1, involves air oxidation, together with a sequence of choreographed keto/enol tautomerizations and quinone/hydroquinone redox transformations.



Scheme 1. A plausible mechanism for the equilibration of kibelones A–C (1–3).

In the proposed mechanism, kibelone C (3) undergoes air oxidation to yield kibelone B (2). We have demonstrated that this transformation can be synthetically accelerated and driven to completion by using the oxidant FeCl_3 (as measured by HPLC-DAD-MS). It is our hypothesis that kibelone B (2) is suitably configured to undergo an acid-mediated double keto/enol tautomerization to yield an unstable quinone-methide intermediate, which can in turn undergo a third keto/enol tautomerization to yield the hydroquinone 10 in which ring C has aromatized. The hydroquinone 10 is presumed to be highly susceptible to oxidation as it was not detected in any *Kibdelosporangium* sp. extracts or fractions, nor was it detected in the equilibrium mixtures derived from either kibelones B or C. It is proposed that the intermediate hydroquinone 10 undergoes oxidation by two possible routes. The first, and most favored route occurs by a quinone/hydroquinone redox transformation between stoichiometric amounts of the quinone kibelone B (2) and the hydroquinone 10, to yield the hydroquinone kibelone C (3) and the quinone kibelone A (1). This reversible redox transformation would establish a steady-state equilibrium between 2/10 and 3/1 based on the respective oxidation potentials of the quinone/hydroquinone pairs. The hydroqui-

none 10 could also undergo air oxidation directly to 1. As this latter air oxidation process would not sustain an equilibrium outcome, under the equilibrium conditions employed it is presumably disfavored over a redox quinone/hydroquinone process. The proposed mechanism also explains the stability of kibelone A (1), in so far as aromatic stabilization of ring C in 10 ensures that the sequence of keto/enol transformations leading from 2 to 10 is irreversible, and any redox transformation involving 1 and 10 would not lead to new chemical entities. Supportive of the stability of kibelone A (1), treatment of 1 with sodium dithionite results in quantitative transformation to the hydroquinone 10, but does not lead to other kibelones, as determined by ^1H NMR spectroscopic analysis (see the Supporting Information).

In the absence of crystals suitable for X-ray analysis, and in an attempt to assign absolute stereochemistry, we acquired the CD spectrum for kibelone A (1). Unfortunately, attempts to assign an absolute stereochemistry to 1 based on the application of empirical CD rules (for example, the octant rules) proved problematic, due to the complexity of the conjugated system and the absence of CD analyses on suitable model compounds. The absolute stereochemistry of the kibelones remains unassigned at this time, and will most likely require either the preparation of suitable crystalline derivatives for X-ray analysis or total asymmetric synthesis, or perhaps quantum mechanical calculations aimed at simulating either CD or optical properties.

Our study also recovered a higher molecular weight kibelone that was identified as kibelone B rhamnoside (5). HRESI(+)-MS analysis of 5 revealed a pseudo molecular ion consistent with a molecular formula ($\text{C}_{35}\text{H}_{36}^{35}\text{ClNO}_{14}$, $\Delta\text{mmu}=1.8$) requiring 18 DBE. The ^1H and ^{13}C NMR spectroscopic data for 5 were consistent with a 6-deoxymonosaccharide glycoside of kibelone B (2). Indeed, the NMR spectroscopic data for the aglycone portion of this molecule (see the Supporting Information) were in full agreement with that previously recorded for kibelone B (2), with the only significant differences being deshielding of H-11 ($\Delta\delta=0.1$ ppm) and the appearance of additional sugar resonances. The NMR resonances attributed to the sugar subunit in 5 included an anomeric centre ($\delta_{\text{H}}=4.87$, $\delta_{\text{C}}=97.7$ ppm), four oxymethines ($\delta_{\text{H}}=3.74$, $\delta_{\text{C}}=70.4$ ppm; $\delta_{\text{H}}=3.52$, $\delta_{\text{C}}=70.6$ ppm; $\delta_{\text{H}}=3.22$, $\delta_{\text{C}}=72.0$ ppm; and $\delta_{\text{H}}=3.49$, $\delta_{\text{C}}=68.8$ ppm), and a secondary methyl ($\delta_{\text{H}}=1.15$, $\delta_{\text{C}}=17.9$ ppm), consistent with a 6-deoxypyranose. Values of $J(2',3')=1.6$, $J(3',4')=9.3$, and $J(4',5')=9.1$ Hz further defined the sugar as rhamnose. A gHMBC correlation from H-11 ($\delta_{\text{H}}=4.01$ ppm) to the anomeric carbon atom ($\delta_{\text{C}}=97.7$ ppm) confirmed 5 to be a C-11 rhamnoside.

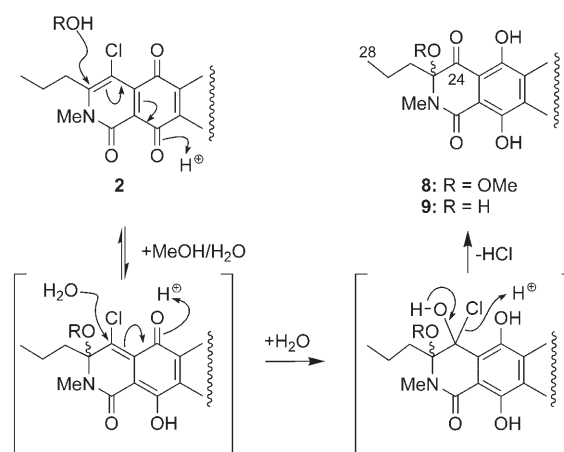
As a measure of the challenge associated with the assignment of the glycosidic linkage stereochemistry, a 1982 study^[6] on rhamnose sugars calculated identical dihedral angles and $J(1,2)$ values for both α - and β -rhamnosylated flavonides. This observation notwithstanding, in general^[7] α -rhamnopyranosides possess a value of $J(1,2)=0.6$ –3.5 Hz (eq,eq), while for β -rhamnopyranosides $J(1,2)=1.5$ –5.8 Hz

(ax,eq). In light of this, a kibdelone B rhamnoside (**5**) $J(1',2')=0.98$ Hz tentatively favors an α -rhamnopyranoside stereochemistry. An analysis of the ^1H NMR coupling constants associated with ring F resonances for **5** ($J(10,11)=3.6$, $J(11,12a)=12.6$, $J(12a,12b)=13.0$, $J(12a,13)=4.0$, and $J(12b,13)=1.8$ Hz) suggested the same relative stereochemistry as assigned above for kibdelones A–C (**1–3**). The absolute stereochemistry of the rhamnose residue, and the relative stereochemistry between rhamnosyl and polyketide subunits in **5**, remain unassigned at this time. Although kibdelone A rhamnoside (**4**) and kibdelone C rhamnoside (**6**) were not isolated directly from the *Kibdelosporangium* sp. extract, we did observe that the glycoside **5** (just as with its corresponding aglycone **2**) underwent equilibration in MeOH at 40°C to give a mixture consistent with **4–6** as determined by HPLC-DAD-MS data. Armed with this data we reanalyzed the HPLC-DAD-MS data for the *Kibdelosporangium* sp. extract and fractions and were able to identify the natural occurrence of all three kibdelone rhamnosides (**4–6**). This observation confirms that both kibdelone aglycones and glycosides are prone to the equilibration as proposed in Scheme 1.

HRESI(+)MS analysis of a minor kibdelone **7** revealed a pseudo molecular ion consistent with a molecular formula ($\text{C}_{29}\text{H}_{22}^{35}\text{ClNO}_{10}$, $\Delta\text{mmu}=0.7$) suggestive of a didehydro kibdelone A (**1**) analogue. The ^1H and ^{13}C NMR spectroscopic data for **7** were remarkably similar with that for **1** with the only significant differences being associated with ring F resonances, namely, the absence of a hydroxy methine, a significant downfield shift of the diastereotopic methylene resonances (H-12a, $\delta_{\text{H}}=3.05$ ppm; and H-12b, $\delta_{\text{H}}=2.70$ ppm), and COSY correlations that defined an isolated spin system involving H-10 ($\delta_{\text{H}}=4.97$ ppm), H-11 ($\delta_{\text{H}}=4.14$ ppm), and H₂-12. These comparisons confirmed **7** as an oxidized analogue of kibdelone A (**1**) bearing a C-13 ketone functionality. Further support for 13-oxokibdelone A (**7**) was obtained from the gHMBC data, which revealed a key correlation from H₂-12 to C-13 ($\delta_{\text{C}}=191.3$ ppm). Analysis of the ring F ^1H NMR coupling constants ($J(10,11)=2.8$, $J(11,12a)=12.9$, $J(11,12b)=4.3$, and $J(12a,12b)=16.5$ Hz) suggested a common relative stereochemistry with kibdelones A–C (**1–3**).

HRESI(+)MS analysis of another minor kibdelone analogue **8** revealed a pseudo molecular ion consistent with a molecular formula ($\text{C}_{30}\text{H}_{31}\text{NO}_{12}$, $\Delta\text{mmu}=-0.3$) lacking the chlorine substituent common to the kibdelones described above, and requiring 16 DBE. Particularly noteworthy in the ^1H NMR spectroscopic data for **8** were resonances for an O–Me ($\delta_{\text{H}}=3.08$, $\delta_{\text{C}}=51.3$ ppm) and a ketone carbonyl ($\delta_{\text{C}}=196.2$ ppm), in addition to a suite of resonances in common with those reported for kibdelone C (**3**). The appearance of a deshielded quaternary sp^3 carbon atom (C-25, $\delta_{\text{C}}=92.8$ ppm) linking through gHMBC correlations to H₂-26 ($\delta_{\text{H}}=2.03$ ppm), an O–Me ($\delta_{\text{H}}=3.08$ ppm), and the typical kibdelone lactam N–Me ($\delta_{\text{H}}=3.03$ ppm) was indicative of O–Me substitution at C-25. Placement of the ketone functionality as shown was confirmed by gHMBC correla-

tions from H₂-26 to C-24 ($\delta_{\text{C}}=196.2$ ppm). The presence of rings B, C, D, E, and F in common with kibdelone C (**3**) was established by direct NMR spectroscopic comparisons and 2D NMR analysis (see the Supporting Information). Assignment of **8** as 25-methoxy-24-oxokibdelone C raises the possibility that **8** was an artifact of kibdelone B (**2**), generated by solvolysis during isolation and handling. A plausible mechanism for this solvolysis is shown in Scheme 2. In this mecha-



Scheme 2. A plausible mechanism for the formation of 25-methoxy-24-oxokibdelone C (**8**) and 25-hydroxy-24-oxokibdelone C (**9**) from the solvolysis of kibdelone B (**2**).

nism C-25 undergoes nucleophilic addition by MeOH to yield a methoxylated quinone methide. Subsequent nucleophilic addition by H₂O to C-24 of the quinone methide returns an α -chloro alcohol that undergoes the irreversible loss of HCl to yield 25-methoxy-24-oxokibdelone C (**8**). A failure to observe products from the addition of MeOH to C-24 in **2** most likely illustrates the inability of the resulting methylated α -chloro alcohol intermediate to advance through loss of HCl to a stable ketone, preferring instead to lose MeOH and revert to the chloro quinone methide.

In a separate fraction, a very minor but structurally related kibdelone analogue **9** was found to co-occur with **8**. The analogue **9** was more polar than **8**, possessed an identical UV-visible spectrum (as determined by DAD), and displayed a molecular weight 14 amu less than that for **8**. While a paucity of sample precluded a complete spectroscopic characterization, we tentatively propose that **9** is 25-hydroxy-24-oxokibdelone C, and arises through nucleophilic addition of H₂O to C-25 (Scheme 2). Thus, we propose that both **8** and **9** could be artifacts generated in aqueous MeOH solutions by the presence of acidic cometabolites (for example, hydroquinones). This being the case, both **8** and **9** are expected to be racemic at C-25.

To further explore our capacity to prepare kibdelone analogues, with a view to possible future structure activity relationship (SAR) investigations, we assessed the effect of halide salts on kibdelone production. A spore suspension of *Kibdelosporangium* sp. (MST-108465) was used to inoculate

ISP2 agar containing additions of a) 0.5% NaBr, b) 0.5% NaCl, or c) no additional halide salts. After incubation at 28°C for seven days, these cultures were extracted with MeOH and the crude extracts were analyzed by HPLC-DAD-MS. Whereas cultures grown under all conditions (a–c) produced kibdelones as expected, the culture grown in the presence of NaBr yielded new metabolites tentatively identified as bromokibdelones.

It is hypothesized that the bromokibdelones detected in this study represent kibdelones A–C in which the C-24 chloro substituent has been replaced by a bromo moiety. Comparative retention times and ESI(±)MS data for kibdelones A–C (**1–3**) and the putative bromokibdelones A–C are listed in Table 3. This analysis, together with an excellent

Table 3. Comparative HPLC-MS-DAD data for kibdelones A–C (**1–3**)^[a] and the putative bromokibdelones A–C.^[b]

	Kibdelones			Bromokibdelones		
	<i>t_R</i> [min]	[M+H] ⁺	[M–H] [–]	<i>t_R</i> [min]	[M+H] ⁺	[M–H] [–]
A	11.2	582/584	580/582	A	11.4	626/628
B	10.8	584/586	582/584	B	11.0	628/630
C	11.5	586/588	584/586	C	11.5	630/632

[a] The ³⁵Cl/³⁷Cl isotope ratio was 3:1. [b] The ⁷⁹Br/⁸¹Br isotope ratio was 1:1.

comparison of the distinctive UV-visible spectra (extracted from the HPLC-DAD-MS traces) for kibdelones A–C with those for the putative bromokibdelones A–C, supported the premise that NaBr augmented media yielded bromokibdelones. While only carried out at an analytical scale (single Petri dish), this study demonstrates our ability to manipulate *Kibdelosporangium* sp. biosynthesis, to access unnatural kibdelone analogues for future SAR investigations.

While the kibdelones possess novel molecular structures, they do belong to a class of polyketides populated by a limited selection of related microbial metabolites, many of which display significant antibacterial, antifungal, antiparasitic, and/or anticancer activity (Table 4). These include the antiparasitic,^[8] antibacterial, and antifungal,^[9,19] albufungins

Table 4. Biological properties^[a] for the kibdelones and structurally related microbial metabolites.

Compound Class	Ab ^[b]	Af ^[c]	Nt ^[d]	Ap ^[e]	Ac ^[f]	Ref.
kibdelones	X		X		X	
citreamicins	X				X	[12,17]
kigamicins	X				X	[15,16]
simaomicins	X			X		[14,18]
albufungins	X	X	X			[8,19]
actinoplanones	X	X			X	[10,11]
Sch54445/56036/42137		X				[20–22]
cervinomycins	X					[23,24]
xantholipins					X	[2,25]
lysolipins					X	[26,27]

[a] X indicates known “areas” of biological activity. Assays against each target “area” differ between structure classes, and as such comparisons should be viewed as indicative, not qualitative. [b] Antibacterial. [c] Antifungal. [d] Nematocidal. [e] Antiprotozoan. [f] Anticancer.

from *Actinomyces* sp, the antibacterial, antifungal,^[10] and antitumor^[11] actinoplanones from an *Actinoplane* sp., and the antitumor^[12] and antibacterial^[13] citreamicins from *Micromonospora citrea*. Xantholipin from a *Streptomyces* sp. and simaomicin from *Actinmadura madurea* are related polyketides that are known to inhibit HSP47 gene expression^[2] and bleomycin-induced G2 cell cycle arrest,^[14] respectively. The anticancer kigamicins from an *Amycolatopsis* sp.^[15,16] are the most recently published example of this structure class.

All the polyketide analogues listed in Table 4 differ structurally from the kibdelones either by ring F aromatization (citreamicin), additional acetal rings (actinoplanones, simaomicin, albufungins and xantholipins), and/or different regiochemistry. Although the activity profiles displayed in Table 4 are not suitable for quantitative comparison (for example, not all compounds underwent the same assays), the diversity of biological profiles does suggest a range of pharmacophores—with the kibdelones possessing a particularly potent and selective pharmacophore.

In our in-house assays, (MST) kibdelones A–C (**1–3**) displayed a common biological profile (Table 5), exhibiting selective Gram +ve antibacterial (*Bacillus subtilis*), and

Table 5. LD₉₉ [nM] bioassay profiles for kibdelones A–C (**1–3**) and the known polyketide, albufungin.

Compound	<i>H. contortus</i>	<i>E. coli</i>	<i>B. subtilis</i>	<i>C. albicans</i>	NS-1
1	0.67	2.7	0.084	– ^[a]	0.041
2	2.2	– ^[a]	0.13	– ^[a]	0.067
3	8.5	– ^[a]	0.13	– ^[a]	0.13
albufungin	1.2	– ^[a]	1.2	≤0.02	≤0.01

[a] Indicates inactive.

potent nematocidal (*Haemonchus contortus*), and cytotoxic (NS-1) activity, while displaying variable activity against Gram -ve bacteria (*Escherichia coli*) and no activity against fungi (*Candida albicans*). The cytotoxic properties of the kibdelones were also evaluated in vitro against a range of human tumors both in house (IMB), under contract (QIMR), and by the NCI in vitro 60-cell panel assays (NCI). Selected data for kibdelones A–C (**1–3**) shown in Table 6 reveal these metabolites as potent and selective cy-

Table 6. GI₅₀ [nM] for kibdelones **1–3** and **5** against selected human tumor cell lines.^[a]

Cell line	1	2	3	5
SR (leukemia)	1.2	1.7	<1.0	219
NCI-H322M (nonsmall cell lung)	1.3	2.3	<1.0	794
HCC-2998 (colon)	3.0	<1.0	<1.0	224
SF-539 (CNS)	1.4	3.2	3.0	479
SK-MEL-5 (melanoma)	1.7	3.1	<1.0	170
SK-OV-3 (ovarian)	3.2	3.6	<1.0	603
SN12C (renal)	<1.0	3.6	<1.0	389
DU145 (prostrate)	3.1	3.0	1.4	537
MCF7 (breast)	5.0	3.5	<1.0	324

[a] Screening carried out against the NCI in vitro 60-cell panel assays (2 d, 10^{–5} M).

tototoxic agents. By contrast the rhamnoside **5**, the oxo analogue **7**, and the methanolysis product **8**, were all significantly less cytotoxic.

Application of the NCI COMPARE analysis to kibdelones A–C (**1–3**), by using GI₅₀ and TGI datasets, against both known anticancer agents and natural product libraries, revealed a number of hits with Pearson's coefficients in the range 0.5–0.7. However, the mean graphs for these hits did not reveal a compelling case that the kibdelones operate by a known anticancer mode-of-action. This observation taken together with the biological profiles displayed in Tables 4 and 5 suggests a biological/anticancer mode-of-action for the kibdelones that is distinct from structurally related polyketides.

Conclusion

The kibdelones represent the first examples from the extended family of biosynthetically related compounds (as listed in Table 4) to be submitted to the NCI screening program—and their sub-nM activity against a selection of human tumor cell lines suggests that further investigation into this structure class is warranted. Although we cannot comment further on the biological mode-of-action of the kibdelones at this time, we view the kibdelones as an exciting new anticancer lead deserving of further studies, aimed at defining the *in vivo* anticancer efficacy and mode-of-action.

Experimental Section

General procedures: High-performance liquid chromatography (HPLC) was performed by using an Agilent 1100 series separations module, Agilent 1100 series diode array, polymer laboratories PL-ELS1000 evaporative light scattering detector (ELSD), and Agilent 1100 series fraction collector and running ChemStation Rev.9.03 A with Purify version A.1.2 software or Rev.10.02 A. Preparative HPLC was carried out on a system consisting of two Shimadzu LC-8 A preparative liquid chromatographs with static mixer, Shimadzu SPD-M10 AVP diode array detector (DAD) and Shimadzu SCL-10 AVP system controller. Standard analytical HPLC conditions refer to 1 mL min⁻¹ gradient elution from 90% H₂O/MeCN (0.05% HCOOH) to MeCN (0.05% HCOOH) over 15 min, followed by a 5 min flush with MeCN on a 5 μm Zorbax Stable Bond C₈ 150 × 4.6 mm column unless otherwise specified. ¹H and ¹³C NMR spectroscopic experiments were performed on a Bruker Avance 600 spectrometer, in [D₆]DMSO (referenced to residual ¹H signals in the deuterated solvent, and *J* values in Hz). ESI(±)MS data were acquired by using an Agilent 1100 series MSD. High-resolution (HR) ESIMS measurements were obtained on a Finnigan MAT 900 XL-Trap instrument with a Finnigan API III source. Chiroptical measurements ([α]_D) were performed on a Jasco P-1010 intelligent remote module-type polarimeter in a 100 by 2 mm cell (units 10⁻¹ deg cm² g⁻¹), while ultraviolet (UV) absorption spectra were obtained by using a CARY3 UV-visible spectrophotometer (units ε-dm³ mol⁻¹ cm⁻¹).

Collection and identification: MST-108465 was isolated from a soil sample collected from a timber woolshed 15 km north of Port Augusta in South Australia in 1996. Analysis of the nonpolar secondary metabolites produced by the culture identified the presence of a series of metabolites with unusual UV spectra. 16S rRNA analysis identified MST-108465 as belonging to the Pseudonocardiaceae and having 98% identity with *Kib-*

delosporangium sp. (aff. *phillipinense*). Comparison with the metabolites produced by known species of *Kibdelosporangium* revealed no secondary metabolites in common with MST-108465. Based on rRNA and metabolite data, MST-108465 is regarded as a novel species, *Kibdelosporangium* sp. (MST-108465).

Fermentation of *Kibdelosporangium* sp.: A spore suspension of MST-108465 was used to inoculate a selection of solid and liquid media to explore the culture's metabolic diversity. The media selected were ISP2 broth, rice flour broth, ISP2 agar, and barley grain. Each media was incubated at 28°C for a range of times based on previous optimal times for other actinomycetes culture. At the conclusion of the incubation, each treatment was processed (see the Supporting Information) to yield the microbial extracts. Of the fermentation conditions, barley grain gave the same distribution of kibdelone-like metabolites but in higher yields than obtained on ISP2 agar. To isolate the remaining minor analogues, a series of solid-phase fermentations using barley were undertaken. Solid fermentations (7 × 500 g barley, incubated for 18 d at 28°C) were extracted with methanol (MeOH) (7 × 1.5 L). The extracts were concentrated in vacuo and pooled to give an aqueous residue (2.6 L) and extracted with ethyl acetate (EtOAc, 2.6 L).

Isolation of kibdelones from mixed media culture: The individual extracts from the mixed media fermentation were pooled to provide 4 L of MeOH extract. This extract was concentrated in vacuo to an aqueous residue (500 mL) that was diluted with H₂O to a final volume of 2 L. This cloudy suspension was passed through two parallel C₁₈ solid-phase extraction (SPE) cartridges (2 × 10 g, Varian HF C₁₈), eluting with 50% aqueous MeOH (2 × 80 mL each) followed by elution with 100% MeOH (2 × 80 mL each). HPLC and bioassay confirmed the presence of the activity and nonpolar metabolites in the MeOH fraction. Partition of the pooled MeOH fraction (160 mL) with hexane removed nonpolar fats (134 mg) yielding an enriched active MeOH fraction (875 mg). The MeOH fraction was dissolved in a mixture of DMSO and MeOH and fractionated by preparative HPLC (60 mL min⁻¹ with gradient elution of 70 to 10% H₂O/MeCN over 20 min followed by MeCN for 10 min, through a 5 μm Platinum EPS C₁₈ 50 × 100 mm column). One hundred fractions were collected, concentrated in vacuo, and combined on the basis of analytical HPLC analysis. The most polar of the fractions (18.2 mg) were pooled and fractionated by HPLC (10 mL min⁻¹ isocratic 35% H₂O/MeCN over 20 min through a Phenomenex LUNA C₁₈ 5 μm (2) 250 × 10 mm column), to yield kibdelone A (**1**) (3.2 mg, 0.37% yield), kibdelone B (**2**) (0.28 mg, 0.03% yield), and kibdelone C (**3**) (1.7 mg, 0.19% yield). All yields are calculated relative to the 875 mg MeOH fraction as identified above.

Isolation of kibdelones from barley grain fermentation: The MeOH extracts from the barley grain fermentation were concentrated in vacuo and pooled to give an aqueous residue (2.6 L). This residue was then extracted with EtOAc (2.6 L). The EtOAc was evaporated in vacuo to yield 8 g of an enriched residue. The residue was dissolved in MeOH and diluted with H₂O to approximately 10% and passed through four parallel C₁₈ solid-phase extraction (SPE) cartridges (4 × 10 g, Varian HF C₁₈). The bound metabolites were eluted with 80% MeOH (4 × 80 mL each), followed by elution with 100% MeOH (4 × 80 mL each) and 100% EtOAc (4 × 80 mL each). HPLC and bioassay confirmed the presence of the activity and nonpolar metabolites in the 80% MeOH fraction (4.9 g). Residual amounts of kibdelones remaining in the aqueous phase after EtOAc extraction were recovered by adsorption onto two parallel C₁₈ solid-phase extraction (SPE) cartridges (2 × 10 g, Varian HF C₁₈) and eluted with 100% MeOH (2 × 80 mL each), followed by 100% EtOAc (2 × 80 mL each). HPLC and bioassay confirmed the presence of the activity and nonpolar metabolites in the MeOH and EtOAc fractions. The fractions were pooled to yield 1.5 g of enriched residue. The enriched residues were pooled (6.4 g).

Duplicate batches of the enriched residues (2 × 2 g) were dissolved in a mixture of DMSO and MeOH and then underwent preparative HPLC (60 mL min⁻¹ with a gradient elution of 25 to 55% H₂O/MeCN over 20 min followed by MeCN for 10 min, through a 5 mm Platinum EPS C₁₈ 50 × 100 mm column). One hundred fractions were collected, concentrated in vacuo, and combined on the basis of analytical HPLC analysis. The fractions containing the major kibdelone metabolites were pooled

(248 mg) and fractionated by multiple serial HPLC (10 mL min⁻¹ gradient of 35% H₂O/MeCN to 45% H₂O/MeCN over 20 min through a Phenomenex LUNA C₁₈ 5 μm (2) 250×10 mm column and 2 mL min⁻¹ gradient elution from 70–65% H₂O/MeCN (0.01% TFA) to MeCN (0.01% TFA) over 20 min through a Zorbax stable Bond C₈ 5 μm (2) 250×10 mm column or through a Zorbax Eclipse C₈ 5 μm (2) 250×10 mm column) to yield kibelone A (**1**) (29 mg, 0.60% yield), kibelone B (**2**) (52 mg, 1.1% yield), kibelone C (**3**) (97 mg, 2.0% yield), kibelone B rhamnoside (**5**) (5.2 mg, 1.1% yield), 13-oxo kibelone A (**7**) (0.9 mg, 0.02% yield), and 25-methoxy-24-oxo kibelone C (**8**) (2.8 mg, 0.06% yield). All yields are calculated relative to the active 80% MeOH fraction (4.9 g) from the enriched EtOAc residue, as indicated above.

Biological activity: Antibacterial, antifungal, nematocidal, and cytotoxicity assays were carried out according to previously published methods.^[28] In vitro 60-cell line anticancer assays were carried out at NCI and the details of the method employed can be found on the website, <http://dtp.nci.nih.gov.html>.

Kibelone A (1): Orange solid; $[\alpha]_{\text{D}}^{25} = +72$ ($c=0.01$ in CHCl₃); ¹H and ¹³C NMR (600 and 150 MHz, respectively, [D₆]DMSO, 25 °C, residual solvent): see Table 1; UV/Vis (EtOH): λ_{max} (ϵ) = 447 (sh), 420 (11000), 311 (20000), 254 (24900), 214 nm (24500 mol⁻¹ m³ cm⁻¹); MS (100 kV, ESI): m/z (%): 582/584 (100/40) [M+H]⁺, 580/582 (30/10) [M-H]⁻; HRESIMS: m/z : calcd for C₂₉H₂₄³⁵CINO₁₀Na: 604.0986 [M+Na]⁺; found: 604.0996.

Kibelone B (2): Orange amorphous solid; $[\alpha]_{\text{D}}^{25} = +157$ ($c=0.01$ in CHCl₃); ¹H and ¹³C NMR (600 and 150 MHz, respectively, [D₆]DMSO, 25 °C, residual solvent): see the Supporting Information; UV/Vis (EtOH): λ_{max} (ϵ) = 444 (sh), 402 (9670), 308 (sh), 258 (23800), 208 nm (22000 mol⁻¹ m³ cm⁻¹); MS (100 kV, ESI): m/z (%): 584/586 (100/40) [M+H]⁺, 582/584 (65/22) [M-H]⁻; HRESIMS: m/z : calcd for C₂₉H₂₆³⁵CINO₁₀Na: 606.1143 [M+Na]⁺; found 606.1128.

Kibelone C (3): Yellow amorphous solid; $[\alpha]_{\text{D}}^{25} = +49$ ($c=0.01$ in CHCl₃); ¹H and ¹³C NMR (600 and 150 MHz, respectively, [D₆]DMSO, 25 °C, residual solvent): see the Supporting Information; UV/Vis (EtOH) λ_{max} (ϵ) = 396 (20100), 339 (sh), 308 (sh), 272 (sh), 258 (27500), 217 nm (22800 mol⁻¹ m³ cm⁻¹); MS (100 kV, ESI): m/z (%): 586/588 (100/40) [M+H]⁺, 584/586 (60/22) [M-H]⁻; HRESIMS: m/z : calcd for C₂₉H₂₈³⁵CINO₁₀Na: 608.1299; found: 608.1259.

Reduction of kibelone A (1) to give 10: Kibelone A (0.5 mg) was dissolved in [D₆]DMSO (300 μL) in an NMR tube and a small amount of Na₂S₂O₄ was added. ¹H NMR (600 MHz) experiments were carried out immediately and after 24 h of standing. A color change was observed from orange to greenish yellow, which disappeared with vigorous shaking, suggesting a possible equilibrium between quinone and hydroquinone. For ¹H and ¹³C NMR (600 and 150 MHz, respectively, [D₆]DMSO, 25 °C, residual solvent) as well as complete 2D assignments of compound **10** see the Supporting Information.

Kibelone B rhamnoside (5): Orange amorphous solid; $[\alpha]_{\text{D}}^{25} = +150$ ($c=0.01$ in CHCl₃); ¹H and ¹³C NMR (600 and 150 MHz, respectively, [D₆]DMSO, 25 °C, residual solvent): see the Supporting Information; UV/Vis (EtOH): λ_{max} (ϵ) = 435 (5700), 308 (sh), 258 (16300), 205 nm (18600 mol⁻¹ m³ cm⁻¹); MS (100 kV, ESI): m/z (%): 730/732 (100/40) [M+H]⁺, 728/730 (40/16) [M-H]⁻; HRESIMS: m/z : calcd for C₃₃H₃₆³⁵CINO₁₄Na: 752.1722; found: 752.1740.

13-Oxo kibelone A (7): ¹H and ¹³C NMR (600 and 150 MHz, respectively, [D₆]DMSO, 25 °C, residual solvent): see the Supporting Information; MS (100 kV, ESI): m/z (%): 580 (100/40) [M+H]⁺, 578 (40/15) [M-H]⁻; HRESIMS: m/z : calcd for C₂₉H₂₂³⁵CINO₁₀Na: 602.0832; found: 602.0839.

25-Methoxy-24-oxo kibelone C (8): Yellow amorphous solid; $[\alpha]_{\text{D}}^{25} = +164$ ($c=0.01$ in CHCl₃); ¹H and ¹³C NMR (600 and 150 MHz, respectively, [D₆]DMSO, 25 °C, residual solvent): see the Supporting Information; UV/Vis (EtOH): λ_{max} (ϵ) = 429 (12100), 388 (sh), 317 (sh), 254 (23100), 221 (sh), 208 nm (21200 mol⁻¹ m³ cm⁻¹); MS (100 kV, ESI): m/z (%): 598 (100) [M+H]⁺, 596 (100) [M-H]⁻; HRESIMS: m/z : calcd for C₃₀H₃₁NO₁₂Na: 620.1744; found 620.1740.

25-Hydroxy-24-oxo kibelone C (9): Structure determination was based on HPLC-DAD-MS and comparison to **8**. MS (100 kV, ESI): m/z (%): 584 (60) [M+H]⁺, 582 (100) [M-H]⁻.

Interconversion of kibelones A–C: Kibelones A–C (**1–3**) and kibelone B rhamnoside (**5**) were heated at 40 °C in MeOH (upto 24 h) while monitoring by HPLC-DAD-MS using standard analytical conditions (see the Supporting Information).

Acknowledgements

G. MacFarlane (Chemistry, UQ) for acquisition of HRESIMS data, Peter Parson (QIMR), J. Challacombe (IMB, UQ), and John Beutler (NCI, USA) for carrying out in vitro cell line assays and UQ for a travel grant (GSRTA) to RR. This research was partially funded by the Australian Research Council.

- [1] E. Lacey, S. Tennant, *Microbiol. Australia* **2003**, *24*, 34–35.
- [2] Y. Terui, Y. Chu, J.-Y. Li, T. Ando, H. Yamamoto, Y. Kawamura, Y. Tomishima, S. Uchida, T. Okazaki, E. Munetomo, T. Seki, K. Yamamoto, S. Murakami, A. Kawashima, *Tetrahedron Lett.* **2003**, *44*, 5427–5430.
- [3] K. Kobayashi, C. Nishino, J. Ohya, S. Sato, T. Mikawa, Y. Shiobara, M. Kodama, *J. Antibiot.* **1988**, *41*, 502–511.
- [4] K. Kobayashi, C. Nishino, J. Ohya, S. Sato, T. Mikawa, Y. Shiobara, M. Kodama, *J. Antibiot.* **1988**, *41*, 741–750.
- [5] G. T. Carter, J. J. Goodman, M. J. Torrey, D. B. Borders, S. J. Gould, *J. Org. Chem.* **1989**, *54*, 4321–4323.
- [6] G. G. Zapesochnaya, *Khim. Prir. Soedin.* **1982**, 695–709.
- [7] J.-F. Hu, D. Wunderlich, I. Sattler, A. Hartl, I. Papastarou, S. Grond, S. Grabley, X.-Z. Feng, R. J. Thiericke, *Antibiotica* **2000**, *53*, 944–953.
- [8] C. Kempter, U. Roos, F. Schroeder, E. Lacey, J. H. Gill, K. Heiland, Albofungin and chloroalbofungin as antihelmintics, 2001-EP67822001095909, 20010615, **2001**.
- [9] A. I. Gurevich, M. N. Kolosov, V. V. Onoprienko, I. D. Ryabova, *Antibiotiki* **1974**, *19*, 827–830.
- [10] C. Nishino, K. Kobayashi, T. Mikawa, Agrochemical fungicides containing polycyclic xanthenes for *Pyricularia oryzae*, 88-3496201211510, 19880219, **1989**.
- [11] C. Nishino, K. Kobayashi, M. Kikuchi, H. Ogishi, T. Mikawa, J. Oya, S. Sato, K. Hirayama, Polycyclic xanthone antibiotics with antitumor and antifungal activity and their manufacture with *Actinoplanes*, 87-1996863188683, 19870130, **1988**.
- [12] J. L. Fernandez-Puentes, L. M. Canedo-Fernandez, D. Garcia-Gravalo, J. Perez-Baz, F. Romero-Millan, F. Espliego-Vazquez, Use of citreamicins as antitumor agents, 2001-GB21482001087283, 20010517, **2001**.
- [13] S. M. Qadri, H. Saldin, Y. Ueno, S. R. al-Ballaa, *Chemotherapy* **1992**, *38*, 395–398.
- [14] M. Arai, H. Sato, H. Kobayashi, M. Suganuma, T. Kawabe, H. Tomoda, S. Omura, *Biochem. Biophys. Res. Commun.* **2004**, *317*, 817–822.
- [15] S. Kunimoto, H. Esumi, J. Lu, H. Naganawa, M. Hamada, Novel antitumor antibiotics, kigamicin A–E, and their manufacture and medical compositions, 2002-3020062004137175, 20021016, **2004**.
- [16] S. Kunimoto, T. Someno, H. Esumi, Manufacture of antibacterial and antitumor antibiotics, kigamicinons (kigamicin aglycon and its derivatives), from kigamicins and pharmaceutical compositions containing them, 2004–2736792006089390, 20040921, **2006**.
- [17] G. T. Carter, J. J. Goodman, D. P. Labeda, Antibiotic LL-E 19085 alpha manufacture with *Micromonospora citrea*, 90-102830442003, 19900213, **1991**.
- [18] T. M. Lee, G. T. Carter, D. B. Borders, *J. Chem. Soc. Chem. Commun.* **1989**, 1771–1772.

- [19] A. I. Gurevich, M. G. Karapetyan, O. A. Kiseleva, T. A. Koloditskaya, M. N. Kolosov, V. V. Onoprienko, B. V. Rozynov, I. D. Ryabova, G. M. Smirnova, *Antibiotiki* **1972**, *17*, 771–774.
- [20] R. Cooper, I. Truumees, I. Gunnarsson, D. Loebenberg, A. Horan, J. Marquez, M. Patel, V. Gullo, M. Puar, *J. Antibiot.* **1992**, *45*, 444–453.
- [21] M. Chu, I. Truumees, R. Mierzwa, J. Terracciano, M. Patel, P. R. Das, M. S. Puar, T.-M. Chan, *Tetrahedron Lett.* **1998**, *39*, 7649–7652.
- [22] M. Chu, I. Truumees, R. Mierzwa, J. Terracciano, M. Patel, D. Loebenberg, J. J. Kaminski, P. Das, M. S. Puar, *J. Nat. Prod.* **1997**, *60*, 525–528.
- [23] A. Nakagawa, S. Omura, K. Kushida, H. Shimizu, G. Lukacs, *J. Antibiot.* **1987**, *40*, 301–308.
- [24] S. Omura, Y. Iwai, K. Hinotozawa, Y. Takahashi, J. Kato, A. Nakagawa, A. Hirano, H. Shimizu, K. J. Haneda, *Antibiotica* **1982**, *35*, 645–652.
- [25] Y. Terui, Z. X. Chen, T. Ando, Y. W. Chu, A. Kawashima, Antitumor xanthone compounds manufacture with *Streptomyces* and chemical synthesis, 2001-JP85662002027010, 20010928, **2002**.
- [26] N. Kanbayashi, Y. Kadota, A. Ookura, H. Suda, M. Okanishi, *Streptomyces* in manufacturing anticancer lysolipin X and/or I, 90-13188204026625, 19900522, **1992**.
- [27] Y. Hayakawa, M. Kamimasahara, Y. Toda, Anticancer agents containing lysolipin X and its manufacture with *Streptomyces platensis*, 88-32014602167092, 19881219, **1990**.
- [28] R. J. Capon, R. Ratnayake, M. Stewart, E. Lacey, S. Tennant, J. H. Gill, *Org. Biomol. Chem.* **2005**, *3*, 123–129.

Received: August 28, 2006
Published online: November 8, 2006